

APPROXIMATE MAXIMUM LIKELIHOOD ESTIMATORS FOR POSITION AND ENERGY IN SCINTILLATION CAMERAS

Neal H. Clinthorne, Chor-yi Ng, and W. Leslie Rogers

Division of Nuclear Medicine and Bioengineering Program
3480 Kresge III Box 0552
The University of Michigan, Ann Arbor, MI 48109-0552
clinthor@petclu.petnet.med.umich.edu

ABSTRACT

It is often assumed that the photon arrival process incident on the photodetector array in a scintillation camera is Poisson, conditioned on the location and energy of the incident gamma-ray. A simple experiment, in which the covariance between the sensor outputs is empirically determined demonstrates that the observations are *not* independent conditioned merely on location and energy. We assume that this lack of independence arises from random parameters influencing the Poisson intensity or photodetector responses. Because, these responses can be difficult to either model or measure as a function of the nuisance parameters, we develop two simple approximations to the ideal maximum likelihood estimator for location and energy.

1. BACKGROUND

A scintillation camera measures the position and energy of incoming γ -ray photons and is used in a variety of applications ranging from γ -ray astronomy to nuclear medicine. Incident γ -rays interact in a scintillation crystal to produce a weak light flash, which spreads throughout the crystal and is subsequently converted to a vector of electrical signals via an array of photodetectors (usually photomultipliers). From this vector, both the x-y location and the energy of each incoming γ -ray can be estimated.

It is often assumed that the number of scintillation photons impinging on each photodetector are Poisson distributed conditioned on the x-y location and energy of the γ -ray. This idea naturally leads to the use of a maximum likelihood estimator for the Poisson model [1], viz.

$$\hat{\theta}_{ML} = \arg \max_{\theta} f(\mathbf{y}|\theta)$$

where

$$f(\mathbf{y}|\theta) = \prod_{i=1}^M \frac{e^{-s_i(\theta)} (s_i(\theta))^{y_i}}{y_i!}$$

and where $\mathbf{y} = [y_1, \dots, y_M]^T$ are the photodetector outputs (assuming noiseless gain), $\theta = [\mathbf{x}, \lambda]^T$ (\mathbf{x} being the interaction position and λ the incoming energy), and $\mathbf{s}(\theta) = [s_1(\theta), \dots, s_M(\theta)]^T$ is the vector representing the expected photodetector output for each θ . Maximization is typically performed by solving the following equation for θ

$$\nabla \mathbf{s}(\theta) \text{diag}^{-1}(\mathbf{s}(\theta))(\mathbf{y} - \mathbf{s}(\theta)) = \mathbf{0}, \quad (1)$$

which can be accomplished in real time using specialized hardware [2].

A key assumption in the model is independence of the noise in the photodetector outputs; however, a simple experiment in which the covariance matrix of the sensor outputs is estimated empirically, demonstrates that the signals are highly correlated, and thus not independent. A sample covariance matrix for one of our systems is

$$\hat{K} = 10^3 \times \begin{bmatrix} 34 & 62 & 3.5 & 0.4 & 0 \\ 62 & 130 & 8.3 & 1.0 & 0 \\ 3.5 & 8.3 & 4.2 & 1.5 & 0.1 \\ 0.4 & 1.0 & 1.5 & 4.0 & 1.5 \\ 0 & 0 & 0.1 & 1.5 & 3.1 \end{bmatrix}. \quad (2)$$

This lack of independence can arise in a variety of ways: for example, it can be the result of a branching process for generating the scintillation light (a cascade of a random scaling and a Poisson process is described in Case I below), or it can be the result of changes in the shape of the response functions $\mathbf{s}(\theta)$ with depth-of-interaction (Case II). We assume that the dependencies are due to random parameters influencing the response functions; and generally, the sensor responses may actually depend upon one or more additional parameters. To correctly model the situation $\mathbf{s}(\theta)$ should

⁰This work was supported by the U.S. DHHS under NIH grants R01 CA54362 and R01 CA32846.

be represented as $\mathbf{s}(\boldsymbol{\theta}; w)$ with corresponding likelihood function

$$f(\mathbf{y}|\boldsymbol{\theta}) = E_w \left[\prod_{i=1}^M \frac{e^{-s_i(\boldsymbol{\theta}; w)} (s_i(\boldsymbol{\theta}; w))^{y_i}}{y_i!} \right], \quad (3)$$

where w represents a random parameter. Ideally, it is desirable to maximize this expression (which averages over the nuisance parameters) with the choice of $\boldsymbol{\theta}$; however, due to the presence of the expectation operator this task can be difficult—especially at rates greater than 10^5 per second.

An alternative to maximizing (3) is to explicitly estimate w as a nuisance parameter using either ML or MAP estimation. In particular, define the joint maximum *a posteriori* (JMAP) estimator as

$$[\hat{\boldsymbol{\theta}}_{\text{JMAP}}, \hat{w}] = \arg \max_{\boldsymbol{\theta}, w} \left[\prod_{i=1}^M \frac{e^{-s_i(\boldsymbol{\theta}; w)} (s_i(\boldsymbol{\theta}; w))^{y_i}}{y_i!} \right] f(w), \quad (4)$$

where $f(w)$ is the prior density for w . Unfortunately, the complete response functions $\mathbf{s}(\boldsymbol{\theta}; w)$ can often be difficult to measure rendering this approach impractical.

2. APPROXIMATE ML ESTIMATORS

Because of the difficulty in measuring the complete response functions, it is reasonable to explore simple approximations to the ML estimator for the pdf given by (3). We consider two approximations: The first is derived from a limiting case for the statistics of the point-process incident on the photosensors and the second from assuming gaussian statistics for the observed photosensor outputs.

2.1. Approximation I

In the limit of low scintillation photon intensity (i.e. $\sum_i s_i(\boldsymbol{\theta})$ small), the statistics of the photosensor observations, conditioned on the incident location and energy, become approximately Poisson-distributed with mean $\bar{\mathbf{s}}(\boldsymbol{\theta}) \triangleq E_w(\mathbf{s}(\boldsymbol{\theta}; w))$. The corresponding estimates $\hat{\boldsymbol{\theta}}_{\text{AML1}}$ under this assumption are solutions to

$$\nabla \bar{\mathbf{s}}(\hat{\boldsymbol{\theta}}_{\text{AML1}}) \mathbf{K}_1^{-1}(\hat{\boldsymbol{\theta}}_{\text{AML1}}) (\mathbf{y} - \bar{\mathbf{s}}(\hat{\boldsymbol{\theta}}_{\text{AML1}})) = 0, \quad (5)$$

where $\mathbf{K}_1^{-1}(\boldsymbol{\theta}) \triangleq \text{diag}^{-1}(\bar{\mathbf{s}}(\boldsymbol{\theta}))$. We refer to estimates satisfying (5) as AML1 estimates. This approximation has the advantage of only requiring knowledge of the mean sensor outputs conditioned on $\boldsymbol{\theta}$, which are straightforward to measure empirically. Given the nature of the inherent assumptions, we might expect best performance in the low-intensity regime.

2.2. Approximation II

An alternative approximation is derived by assuming the photosensor statistics are Gaussian-distributed with log-likelihood

$$\ln f(\mathbf{y}|\boldsymbol{\theta}) = -\frac{1}{2}(\mathbf{y} - \bar{\mathbf{s}}(\boldsymbol{\theta}))^T \mathbf{K}_2^{-1}(\boldsymbol{\theta}_o) (\mathbf{y} - \bar{\mathbf{s}}(\boldsymbol{\theta})) + C$$

where

$$\begin{aligned} \mathbf{K}_2(\boldsymbol{\theta}_o) &= E_w[E(\mathbf{y}\mathbf{y}^T | w, \boldsymbol{\theta}_o)] \\ &- E_w[E(\mathbf{y} | w, \boldsymbol{\theta}_o)] E_w[E(\mathbf{y}^T | w, \boldsymbol{\theta}_o)] \end{aligned}$$

is the covariance of the sensor outputs at the true (but unknown) $\boldsymbol{\theta}_o$. Forming the least-squares normal equations, and substituting $\mathbf{K}_2(\hat{\boldsymbol{\theta}}_{\text{AML2}})$ for the unknown $\mathbf{K}_2(\boldsymbol{\theta}_o)$, gives

$$\nabla \bar{\mathbf{s}}(\hat{\boldsymbol{\theta}}_{\text{AML2}}) \mathbf{K}_2^{-1}(\hat{\boldsymbol{\theta}}_{\text{AML2}}) (\mathbf{y} - \bar{\mathbf{s}}(\hat{\boldsymbol{\theta}}_{\text{AML2}})) = 0, \quad (6)$$

which is solved to yield AML2 estimates $\hat{\boldsymbol{\theta}}_{\text{AML2}}$. As for the AML1 estimator, knowledge of the complete response functions $\mathbf{s}(\boldsymbol{\theta}; w)$ is not required, and both $\bar{\mathbf{s}}(\boldsymbol{\theta})$ and $\mathbf{K}_2(\boldsymbol{\theta})$ are simple to measure. Moreover, (6) is only moderately more difficult to implement than (5) requiring multiplication at each trial value of $\boldsymbol{\theta}$ by a non-diagonal information matrix.

3. EXAMPLES

We present two brief examples comparing the performance of AML1, AML2, and JMAP estimators. The first demonstrates the equivalence of these estimators for a particular response model; the second, the superiority of AML2 over AML1 estimates for a case in which the responses are strongly dependent on an unknown γ -ray depth-of-interaction.

Case I: Poisson process with random rate

For this example, assume the response functions can be separated into a component depending only on γ -ray energy and one depending only on position, i.e., $\mathbf{s}(\boldsymbol{\theta}) = \lambda g \mathbf{s}(\mathbf{x})$ where g is an i.i.d. random scaling of each event (additionally we assume g is non-negative and bounded).¹ The cascade of any random scaling with a Poisson process results in a covariance of the form:

$$\mathbf{K}_2([\mathbf{x}, \lambda]^T) = \lambda \bar{g} \text{diag}(\mathbf{s}(\mathbf{x})) + \lambda^2 \sigma^2(g) \mathbf{s}(\mathbf{x}) \mathbf{s}^T(\mathbf{x}), \quad (7)$$

¹This approximates the actual case where it is highly likely that the γ -ray will undergo a photoelectric interaction with the release of an energetic electron. This electron generates a random number of secondary ionizations, each of which ultimately produce a random number of scintillation photons.

or a rank-1 modification of the covariance for the purely Poisson problem. Note that all entries are positive, similar to (2).

It is straightforward to show that estimates resulting from the use of the AML1 and AML2 (eqs. (5) and (6), respectively) coincide for all observations \mathbf{y} ; i.e., the null spaces of the matrices

$$\nabla_{\mathbf{x},\lambda}(\lambda\bar{g}\mathbf{s}(\mathbf{x}))\mathbf{K}_1^{-1}([\mathbf{x},\lambda]^T)$$

and

$$\nabla_{\mathbf{x},\lambda}(\lambda\bar{g}\mathbf{s}(\mathbf{x}))\mathbf{K}_2^{-1}([\mathbf{x},\lambda]^T)$$

are identical for all $[\mathbf{x},\lambda]$. This can be seen by using the identity:

$$\begin{aligned}\mathbf{K}_2^{-1} &\equiv \mathbf{K}_1^{-1} + \mathbf{K}_1^{-1}\mathbf{s}\left(\frac{1}{\lambda^2\sigma^2(g)} + \mathbf{s}^T\mathbf{K}_1^{-1}\mathbf{s}\right)^{-1}\mathbf{s}^T\mathbf{K}_1^{-1} \\ &\equiv \mathbf{K}_1^{-1} + \beta\mathbf{1}\mathbf{1}^T\end{aligned}$$

and noting that for all admissible AML1 and AML2 estimates $\mathbf{1}\mathbf{1}^T(\mathbf{y} - \lambda\bar{g}\mathbf{s}(\mathbf{x})) \equiv \mathbf{0}$. Furthermore, these estimators are equivalent to the JMAP estimator defined in (4) if

$$\frac{\partial \ln f(g|\lambda)}{\partial \lambda} = 0 \implies \frac{\partial \ln f(g|\lambda)}{\partial g} = 0.$$

These equivalences do *not* hold, however, if a prior density $f(\lambda)$ on γ -ray energy is used to form MAP estimates.

Case II: Change in response shape with depth

In practice, normally-incident γ -rays do not interact in a single plane within the scintillation crystal but rather at a random depth. The pdf for this depth of interaction is given by

$$f(z|\lambda) = d^{-1}(\lambda)e^{-z/d(\lambda)}, \quad (8)$$

where z is the depth-of-interaction and $d(\lambda)$ is an energy-dependent attenuation length. Unfortunately, the mean sensor response usually depends on this interaction depth; i.e., $\mathbf{s}(\theta) = \mathbf{s}(\theta; z)$.

To illustrate the relative performance of AML1 and AML2 estimators for this application, consider the following example: A linear array of five photodetectors measures the light output from a scintillation crystal, and the shapes of their response functions vary significantly with depth-of-interaction of the γ -ray. Response functions for various source locations are shown for the minimum and maximum depths-of-interaction in Fig. 1.

Results of applying the AML1 (*) and AML2 (o) estimators are shown in Figs. 2 and 3. Use of the AML1 estimator, which is often employed in practice because

of its low complexity, can lead to severe errors in estimates of location (Fig. 2) and energy (Fig. 3) due to both high variance and bias. Application of the AML2 estimator given by (6) results in a significant performance improvement.

For the same response functions, results of applying the AML1 and AML2 estimators, as well as those obtained using the JMAP estimator given by (4) are shown in Figure 4. Results are plotted against varying mean numbers of photons per scintillation pulse for a fixed location and energy ($\mathbf{x} = 37$ mm, $\lambda = 1$). As a practical lower bound for estimates produced by maximizing (3) over θ , we have also shown results for an ML estimator in which the true depth-of-interaction was supplied as a known parameter for each realization. Each point represents 100 independent trials. At low photon rates, all estimators perform nearly equivalently in terms of mean-squared error. At higher rates, however, the sub-optimality of AML1 estimates is readily apparent, as well as the excellent performance of the AML2 estimator relative to the more complex JMAP estimator and to the estimator in which the depth-of-interaction was known *a priori*.

4. CONCLUSION

We have developed two approximations to the likelihood function described by equation (3)—neither require full knowledge of the photodetector response functions. Estimators based on the first approximation are useful when either the light flash produced by a γ -ray interaction is extremely weak, or the shapes of the photodetector responses do not vary significantly with random (and unestimated) parameters. Estimators based on the second approximation, which assumes Gaussian photodetector statistics, perform extremely well relative to the ideal estimator. Moreover, they are only moderately more complex than estimators resulting from the first approximation.

5. REFERENCES

- [1] R.M. Gray and A.M. Macovski, "Maximum *a posteriori* estimation of position in scintillation cameras," *IEEE Trans. Nucl. Sci.*, NS-23:849-52, 1976.
- [2] N.H. Clinthorne, W.L. Rogers, L. Shao, and K.F. Koral, "A hybrid maximum likelihood position computer for scintillation cameras," *IEEE Trans. Nucl. Sci.*, 34:97-101, 1987.

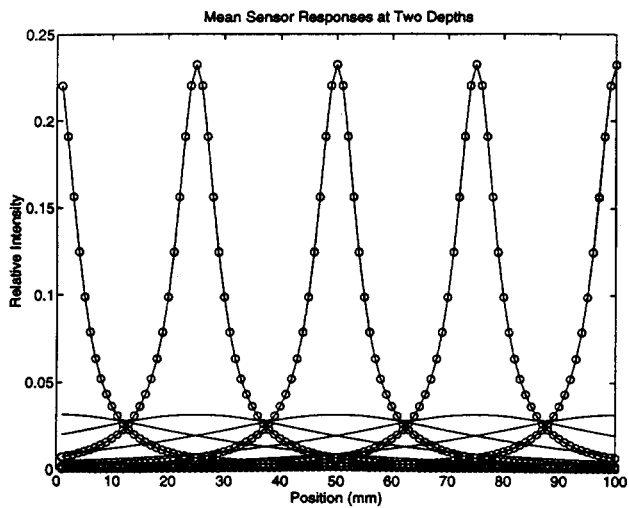


Figure 1: Mean sensor responses for an array of five sensors as a function of γ -ray interaction location at two depths. Maximum depth: (o), Minimum depth: (-).

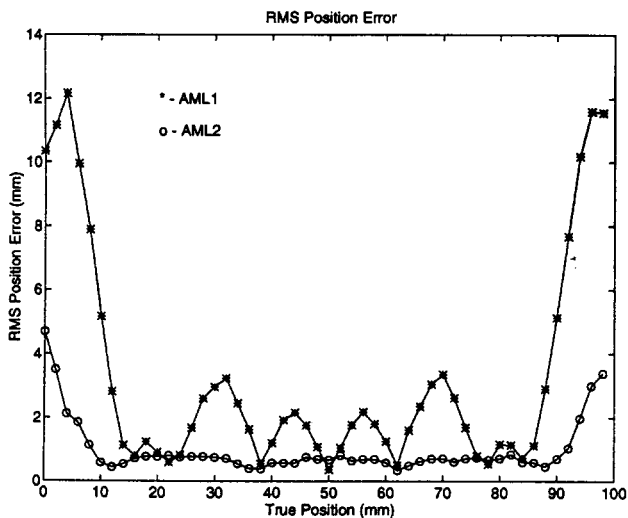


Figure 2: RMS error in position as a function of location for the AML1 and AML2 estimator. Note the improved performance using the AML2 estimator.

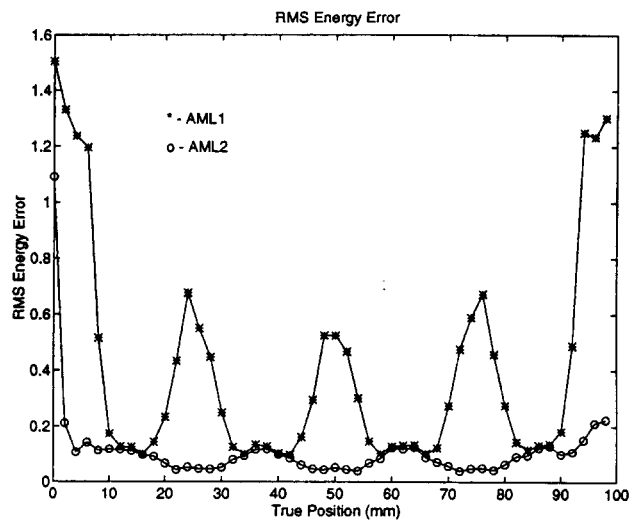


Figure 3: RMS error in energy estimates (true energy \equiv 1) as a function of interaction location. AML2 significantly outperforms AML1 in this case also.

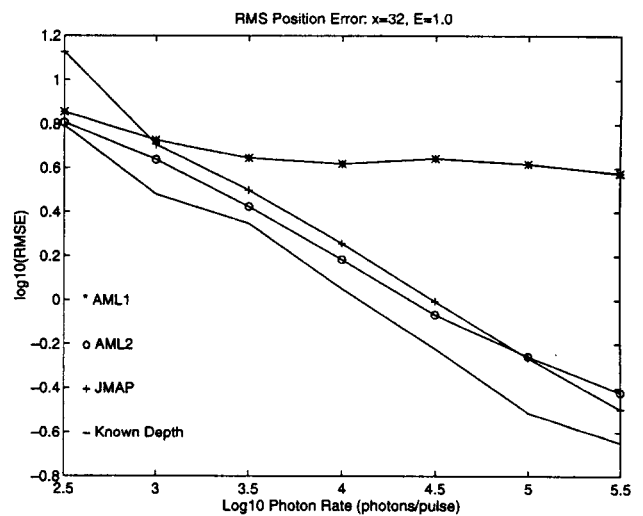


Figure 4: RMS error in position estimates at location 32 mm (true energy \equiv 1) for various mean scintillation pulse intensities. At the higher rates AML2 outperforms AML1, with performance close to that of the JMAP estimator and the ML estimator having knowledge of the depth-of-interaction for each γ -ray.